



**HAL**  
open science

## Cobalt Ferrite Nanoparticles from Single and Multi-Component Precursor Systems

Sanjay Mathur, Christian Cavelius, Karsten Moh, Hao Shen, Jürgen Bauer

► **To cite this version:**

Sanjay Mathur, Christian Cavelius, Karsten Moh, Hao Shen, Jürgen Bauer. Cobalt Ferrite Nanoparticles from Single and Multi-Component Precursor Systems. *Journal of Inorganic and General Chemistry / Zeitschrift für anorganische und allgemeine Chemie*, 2009, 635 (6-7), pp.898. 10.1002/zaac.200900010 . hal-00484129

**HAL Id: hal-00484129**

**<https://hal.science/hal-00484129>**

Submitted on 18 May 2010

**HAL** is a multi-disciplinary open access archive for the deposit and dissemination of scientific research documents, whether they are published or not. The documents may come from teaching and research institutions in France or abroad, or from public or private research centers.

L'archive ouverte pluridisciplinaire **HAL**, est destinée au dépôt et à la diffusion de documents scientifiques de niveau recherche, publiés ou non, émanant des établissements d'enseignement et de recherche français ou étrangers, des laboratoires publics ou privés.



### Cobalt Ferrite Nanoparticles from Single and Multi- Component Precursor Systems

Journal:	<i>Zeitschrift für Anorganische und Allgemeine Chemie</i>
Manuscript ID:	zaac.200900010
Wiley - Manuscript type:	Article
Date Submitted by the Author:	07-Jan-2009
Complete List of Authors:	Mathur, Sanjay; Institute of Inorganic Chemistry Cavelius, Christian; Leibniz Institute of New Materials Moh, Karsten; Leibniz Institute of New Materials Shen, Hao; Department of Inorganic and Materials Chemistry Bauer, Jürgen; Leibniz Institute of New Materials
Keywords:	Cobalt Ferrite, Single-Source Precursor



1  
2  
3  
4  
5  
6  
7  
8  
9  
10  
11  
12  
13  
14  
15  
16  
17  
18  
19  
20  
21  
22  
23  
24  
25  
26  
27  
28  
29  
30  
31  
32  
33  
34  
35  
36  
37  
38  
39  
40  
41  
42  
43  
44  
45  
46  
47  
48  
49  
50  
51  
52  
53  
54  
55  
56  
57  
58  
59  
60

## Cobalt Ferrite Nanoparticles from Single and Multi-Component Precursor Systems

Sanjay Mathur<sup>1,2\*</sup>, Christian Cavelius<sup>2</sup>, Karsten Moh<sup>2</sup>, Hao Shen<sup>1,2</sup> and Jürgen Bauer<sup>2</sup>

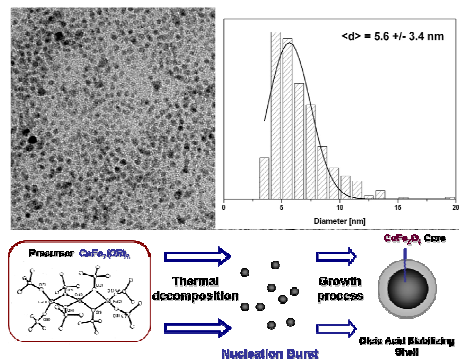
<sup>1</sup>*Department of Inorganic and Materials Chemistry  
University of Cologne, Cologne, D-50931 Germany*

<sup>2</sup>*Leibniz Institute of New Materials, Saarbruecken, D-66123 Germany*

*Dedicated to Prof. Dr. Gerd Meyer as a tribute to his seminal contributions to solid-state and coordination chemistry*

\*Corresponding author: sanjay.mathur@uni-koeln.de

Figure for table of contents



1  
2  
3  
4  
5  
6  
7  
8  
9  
10  
11  
12  
13  
14  
15  
16  
17  
18  
19  
20  
21  
22  
23  
24  
25  
26  
27  
28  
29  
30  
31  
32  
33  
34  
35  
36  
37  
38  
39  
40  
41  
42  
43  
44  
45  
46  
47  
48  
49  
50  
51  
52  
53  
54  
55  
56  
57  
58  
59  
60

## Abstract

Highly crystalline  $\text{CoFe}_2\text{O}_4$  nanoparticles ( $d \sim 5\text{-}6$  nm) were synthesized by thermal decomposition of (i) single molecular precursor  $\text{CoFe}_2(\text{OtBu})_8$  and (ii) stoichiometric mixture of individual metal precursors. The precursors were thermolyzed in a high-boiling solvent (Docosane, bp.  $369^\circ\text{C}$ ) to produce uniformly dispersed cobalt ferrite nanoparticles in the case of molecular precursor, whereas bimodal distribution of nanoparticles was obtained in the multi-source synthesis. TG/DSC and HR-TEM revealed single and multi-step decomposition profiles and differential nucleation steps in the two cases, which influence size dispersion and phase purity.

*Keywords: Cobalt Ferrite, Thermal Decomposition, Single-Source Precursor*

## Introduction

Oxidic magnetic nanocrystals like magnetite, maghemite and cobalt ferrite with superparamagnetic properties have been synthesized by different techniques due to its outstanding and tunable magnetic properties<sup>1</sup>. A wide range of applications basing on iron oxide spinells could be addressed like the use in clinical chemistry<sup>2</sup> as well as ferrofluid for sealing purposes<sup>3</sup>. Beside the essential requirements the greatest challenge for the production of high quality iron oxide systems is the need of a precise control over size, shape and crystallinity because these morphological characteristics allow the engineering of the magnetic properties<sup>4</sup>. Commonly, solution phase methods like the (co)precipitation of the metal ions  $\text{M}^{2+}$  and  $\text{Fe}^{3+}$  in aqueous media by a base or aerosol-mediated techniques are used to produce large quantities of nanoparticles<sup>5</sup>. Even though, these methods are suited for mass production, the controllable synthesis is difficult to achieve and the produced materials are quite often poorly crystalline and polydisperse.

Alternative approaches produce nanoparticles by thermal decomposition of metal organic precursors<sup>6</sup> like iron pentacarbonyl, iron acetylacetonate or iron carboxylates in a high

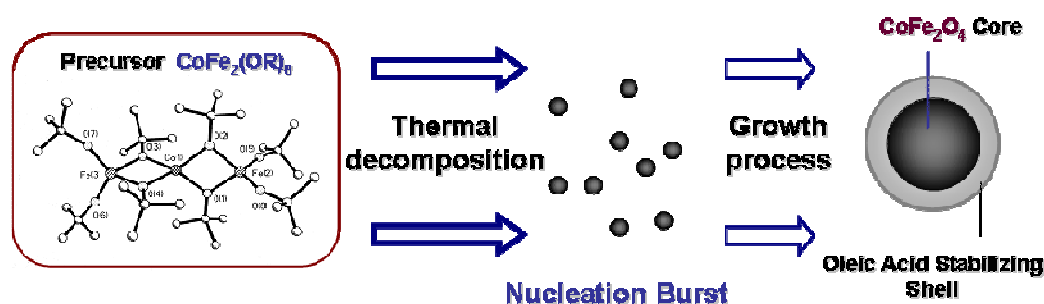
1  
2  
3 boiling organic solvent resulting in highly monodispersive monometallic nanoparticles<sup>7</sup>.  
4  
5 Metal organic alkoxide precursors can decompose at elevated temperatures (around 140 to  
6  
7 340 °C) into metal organic fragments or oxide clusters in a suited high boiling solvent<sup>8</sup>. At a  
8  
9 distinct temperature the precursor decomposes homogeneously into the whole solvent. Many  
10  
11 seeds are formed during this process growing via cross condensation reactions between the  
12  
13 decomposition products which induce a well defined ripening process. This behaviour is used  
14  
15 to produce monodispersive crystalline particles with narrow size distribution<sup>9</sup>.  
16  
17  
18  
19

20 Compared with various other methods like the Sol-Gel-Process it is much easier to  
21  
22 produce huge amounts of deagglomerated particles with moderate time and equipment  
23  
24 consumption. In general, with a suited heating rate there is no concentration gradient of the  
25  
26 metal oxide precursor compound into the solvent, which is a big problem in Sol-Gel-  
27  
28 Processing of particles including the formation of polydisperse seeds, which is only to avoid  
29  
30 by a very precise process control and long / moderate ripening times at soft conditions leading  
31  
32 to amorphous particles which has to be crystallized by other methods like sintering or the  
33  
34 hydrothermal process. Compared with solvothermal or hydrothermal routes powder  
35  
36 production by thermal decomposition is much cheaper because no expensive high-pressure  
37  
38 suited equipment is used and by this way nearly no limitations of up-scaling are given.  
39  
40 Crystallinity, shape and size of the particles can be regulated by temperature and the in situ  
41  
42 capping with stabilizer molecules (mostly long-chain organic mono- or multifunctional  
43  
44 molecules), which enables to produce stable colloids with defined properties<sup>10</sup>. Bimetallic  
45  
46 precursors can be used to form complex metal oxides with a one-step strategy by a very easy  
47  
48 experimental procedure.  
49  
50  
51  
52  
53  
54

55 Nevertheless, removal of the high boiling organic solvent, which is required to obtain  
56  
57 a nanopowder, still remains a challenge. Additionally, the synthesis of particles with  
58  
59 bimetallic oxide phases like  $\text{CoFe}_2\text{O}_4$  is difficult due to the different thermal stability of the  
60  
organic precursors in a multicomponent system. Molecular precursors containing an

appropriate stoichiometry of the required metal ions can be decomposed in a solvent to achieve monodisperse nanoparticles.

In order to control the synthesis of metal oxide nanoparticles, it is important to separate nucleation and growth phases, which can be ideally achieved by decomposition of metal-organic precursors. When the thermal energy available in the reaction medium (solvent) exceeds the chemical bond energy, an abrupt decomposition of the precursor molecules and a single burst of nucleation occurs producing nuclei of similar sizes. By injecting metal-organic precursors in high boiling solvents ( $T > T_{\text{decomposition}}$ ) it is possible to achieve the nucleation of particles in a very short time period, which allows the production of  $\text{CoFe}_2\text{O}_4$  nanoparticles with narrow size distribution (Scheme 1).



Scheme 1. Decomposition of precursor molecules in a high boiling solvent and nucleation and growth steps.

In this paper, we present the synthesis of highly crystalline ferrite powders which is based on the thermal decomposition of a single-source precursor  $\text{CoFe}_2(\text{O}^t\text{Bu})_8$ , which contains the elements ideal Co:Fe ratio for the formation of  $\text{CoFe}_2\text{O}_4$ . The surface of the particles is in-situ capped by oleic acid as long-chain surfactant to keep the particle stable and suspended.

## Experimental

### *Preparation of $\text{CoFe}_2(\text{O}^t\text{Bu})_8$ single-source precursor*

The preparation of  $\text{CoFe}_2(\text{O}^t\text{Bu})_8$  was achieved by salt elimination of sodium iron t-butoxide analogous to the synthesis of  $\text{MgAl}_2(\text{O}^t\text{Bu})_8$  which was reported before<sup>11</sup>. All operations were

1  
2  
3 performed under nitrogen or argon using a modified Schlenk technique. All solvents were  
4  
5 dried via standard methods and stored under sodium wire or molecular sieve.  
6  
7

8 The precursor was synthesized in a 500 ml round bottom flask equipped with  
9  
10 condenser, magnetic stirrer. Typically, 4.44 g (6 mmol) sodium iron t-butoxide was solved in  
11  
12 250 ml of toluene and mixed with a suspension of 0.779 g (3 mmol) cobalt(II) chloride in 50  
13  
14 ml of tetrahydrofuran. After mixing of the two components, the colour turned from green-  
15  
16 brown to deep purple, indicating the formation of the complex. Subsequent heating of the  
17  
18 suspension to reflux for 12 h resulted in the dissolution of the cobalt chloride and the  
19  
20 formation of the paramagnetic complex<sup>12</sup>. After filtration of sodium chloride, evaporation of  
21  
22 the solvent and sublimation of the crude product at 125 °C under vacuum ( $10^{-2}$  mbar) the  
23  
24 purified heterobimetallic compound (Fig. 1) was obtained in yields up to 85 %.  
25  
26  
27  
28  
29  
30

### 31 *Preparation of CoFe<sub>2</sub>O<sub>4</sub> nanocrystals*

32  
33 In a typical procedure, a mixture of 2.54 g (9 mmol) oleic acid and 10g of docosane is heated  
34  
35 to 369 °C under nitrogen followed by the addition of 755 mg (1mmol) of CoFe<sub>2</sub>(O<sup>t</sup>Bu)<sub>8</sub>  
36  
37 dissolved in 2 g Docosane (at 100 °C). Gaseous products indicate the decomposition of the  
38  
39 precursor, which is attended by the almost instantly change in colour from purple to black.  
40  
41 The solution was kept at 369 °C for 30 minutes. to complete the decomposition process and  
42  
43 then cooled down to 80 °C. Addition of ethanol results in precipitation of the nanocrystals  
44  
45 which were purified by standard methods described by Yu et. al.<sup>6</sup>  
46  
47  
48  
49  
50  
51

### 52 *Instrumentation*

53  
54 Structure and phase purity of the synthesized nanoparticles were investigated by X-ray  
55  
56 diffractometry (XRD) with a Phillips X'Pert system (Cu K<sub>α</sub>-radiation,  $\lambda = 0.156056$  nm). A  
57  
58 transmission electron microscope (TEM; Philips CM20) was used to examine particle  
59  
60

1  
2  
3 crystallinity and morphology. Thermogravimetric analyses (DSC-TG) for precursor  
4  
5 decomposition studies were performed under argon at a heating rate of 10 K/min.  
6  
7

## 8 9 10 **Results and Discussion**

11  
12 To obtain non-aggregated nanoparticles, the precursor solution is injected into a high boiling  
13  
14 solvent and a long-chain carboxylic acid as capping agent according to the procedure recently  
15  
16 published by Park<sup>13</sup> for the preparation of iron oxide nanoparticles. For our purposes we  
17  
18 modified the procedure to keep the synthesized Co-Fe alkoxide separated from the capping  
19  
20 agent solution to avoid unwanted hydrolysis of the precursor.  
21  
22  
23

24  
25 After addition of the precursor solution the progress of the reaction can visually be  
26  
27 monitored as the colour of the solution changes from dark purple to black accompanied by the  
28  
29 formation of gaseous decomposition products. Docosane was chosen due to the fact that it  
30  
31 exhibits a very high boiling point of 369 °C, which is necessary to control the decomposition  
32  
33 behavior of the precursor. Experiments at lower temperatures with octadecene as high boiling  
34  
35 solvent only yield poor crystalline and polydispersive products. For a set temperature, no  
36  
37 significant variation of particles size was found by variation of heating rate or concentration  
38  
39 and the particle size and shape are mainly determined by the long chain carboxylic acid acting  
40  
41 as stabilizer. In any cases, an aging step between 30 and 60 minutes is required to obtain  
42  
43  $\text{CoFe}_2\text{O}_4$  crystalline material in high yields > 80 %.  
44  
45  
46  
47

48  
49 Transmission electron microscopy of  $\text{CoFe}_2\text{O}_4$  nanoparticles reveals the high  
50  
51 crystallinity of the as-prepared powder (Fig. 2a). No size-selection process was performed  
52  
53 before the measurement. The nanocrystals are of spherical shape with an average diameter of  
54  
55 ~ 5.6 nm with narrow size distribution. There is no agglomeration of nanoparticles even after  
56  
57 several months of storing in toluene or hexane. The particles are separated from each other  
58  
59 and can be easily precipitated in polar solvents. High-resolution TEM image (Fig. 2b) reveals  
60  
the crystalline features of the particles. The lattice fringe (0.252 nm) can be assigned to <311>

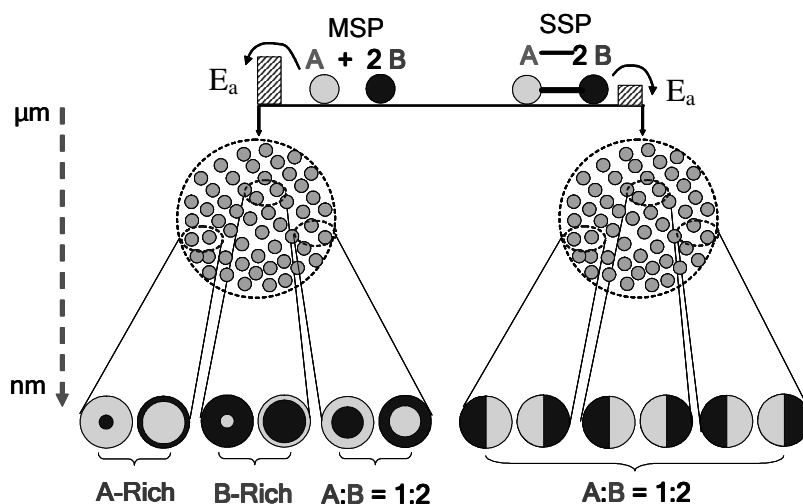
1  
2  
3 lattice plane supported by JCPDS file No. [77-0426]. X-ray diffraction was performed for  
4  
5 nanoparticles aged at 360 °C for 2 h. It confirms the spinel structure and no other phases such  
6  
7 as cobalt- and iron oxides could be identified. By using Scherrer's formula the average  
8  
9 crystallite size was calculated using line broadening of the <400>, <511> and <440> peaks.  
10  
11 The average crystallite size (7.6 nm) determined by XRD pattern is in good agreement with  
12  
13 that of nanoparticles (5.6 nm) estimated from TEM histogram data (Inset, Fig. 2a).  
14  
15

16  
17 The decomposition behavior of the single-source compound has been studied in  
18  
19 comparison to that of the multi-source system,  $\text{Co}(\text{acac})_2$  and  $\text{Fe}(\text{acac})_3$ . To keep the pre-  
20  
21 defined composition and to transfer the ideal Co/Fe ratio at 1:2, a sharp decomposition step of  
22  
23 the precursor is required to prevent earlier fragmentation leading to phase impurities and  
24  
25 polydisperse phases. Although the pyrolysis of the compound is shifted to higher temperatures  
26  
27 one-step decomposition was observed (Fig. 4). After melting of the solid precursor  
28  
29 represented by an endothermic DSC-peak at 213 °C the initial decomposition of  
30  
31  $\text{CoFe}_2(\text{O}^t\text{Bu})_8$  onsets at 260 °C and finishes at 303 °C. At higher temperatures the TG curves  
32  
33 show a stable plateau up to the end of the heating program. For the multi-component system  
34  
35 reduced onset temperatures of  $\text{Co}(\text{acac})_2$  (216 °C),  $\text{Fe}(\text{acac})_3$  (232 °C) and  $\text{Co}(\text{acac})_2 +$   
36  
37  $2\text{Fe}(\text{acac})_3$  mixture (224 °C) were observed. However, the final temperatures, which indicate  
38  
39 the transition to the nano-phase materials are drastically shifted to higher temperatures of 342  
40  
41 and 418.9 °C respectively. Based on these results, the single-source compound seems to be  
42  
43 better suited for particle synthesis in terms of thermal decomposition since the temperature  
44  
45 range is quite small whereas two-stage decomposition of the multi-source system was  
46  
47 observed. This can be explained due to the rather slow degradation of intermediates,  
48  
49 especially in the case of the  $\text{Co}(\text{acac})_2$  precursor. Transmission electron image (Fig. 5) of  
50  
51 nanoparticles obtained from multi-source precursors confirms the two-stage decomposition  
52  
53 behaviour resulting in a bimodal size distribution ( $\langle d_1 \rangle \sim 6.1$  nm;  $\langle d_2 \rangle \sim 21.3$  nm).  
54  
55  
56  
57  
58  
59  
60

1  
2  
3 The intrinsic strength of chemistry to decipher how simple atomic interactions give  
4 rise to complexity can be used to control the arrangement of atoms at multiple length scales,  
5 ranging from molecular to extended solid-state structures. The idea behind the chemical  
6 synthesis of nanomaterials is to transform molecular precursors into materials under retention  
7 of the structural units, which are inherent to the precursor molecule and an integral part of the  
8 solid-state structure<sup>14</sup>. The chemical techniques use direct, often very simple, chemical  
9 reactions in solid, liquid or gaseous state to produce the solid of interest. For instance, solid-  
10 state chemical reactions require grinding, mixing, and subsequent heat-treatments to facilitate  
11 diffusion of atoms or ions to form the final product, which depends on the temperature of the  
12 reaction and the transport across grain boundaries. Compared to diffusion driven multi-  
13 component synthesis, characterized by individual decomposition processes, single molecule-  
14 based synthesis of inorganic nanostructures augments the diffusion and rearrangement  
15 processes and lead to single-phase materials. The later aspect is attributed to precursor  
16 constitution possessing pre-defined metal-ligand structural units relevant for the constitution  
17 of the final nanomaterial. On the other hand, the different compounds present in a reaction-  
18 mixture randomly collide to form various intermediate species inducing phase separation and  
19 element segregation. For instance, a simple mixture of two chemical precursors A and B  
20 (Multi Source Precursor, MSP), to produce the binary system AB, may produce a visibly  
21 homogeneous mixture but the molecular level scenario can be different and despite a correct  
22 global stoichiometry the precursor 'cocktail' may have element segregation and non-ideal  
23 A:B ratios at the nanometer scale that may be carried forward to the end product (Scheme 2).  
24  
25  
26  
27  
28  
29  
30  
31  
32  
33  
34  
35  
36  
37  
38  
39  
40  
41  
42  
43  
44  
45  
46  
47  
48  
49  
50  
51  
52

53 As indicated in Scheme 2, the two-component mixture of Co (A) and Fe (B) acetates,  
54 show multi-step thermal degradation due to individual decomposition profiles of Co and Fe  
55 precursors as confirmed by the TG/DTA analyses of monometallic acetates. Based on this  
56 data, it can be envisaged that the thermal decomposition of such a mixture in high-boiling  
57 solvent results in two nucleation and growth processes, which differ on the reaction time  
58  
59  
60

scales. As a result, the cobalt oxide particles, which are formed (216 °C) first grow to much larger size (ripening), when compared to iron precursors, which decompose later (255 °C) and produces relatively smaller particles.



Scheme 2. Chemical nanotechnology: multi-source vs. single source approaches.

## Conclusions

Pure oleic acid - capped cobalt ferrite nanoparticles were prepared by thermal decomposition of a single-source compound  $\text{CoFe}_2(\text{O}^t\text{Bu})_8$  in a high boiling solvent. A decomposition temperature of 360 – 370 °C was found to be best suited for the synthesis of nanoparticles with around 5 nm in diameter, that are composed of pure cubic  $\text{CoFe}_2\text{O}_4$  spinell phase, as revealed by XRD and HRTEM analysis. TG-DSC measurements were performed for the single- and multi-source system and proved the suitability of the precursor, which decomposes in a single-step process. The obtained particles can be easily dispersed in non-polar solvents like toluene, hexane or chloroform and exhibit an excellent long-term stability. The variation of the particle size has yet to be improved by variation of the carboxylic chain. In the next step, the nanoparticles should be synthesized in a polar high boiling medium with bi-functional groups to make the particles water-soluble. This should promote the application

of the material for biological and medical purposes. A study of the magnetic properties of the particles with different capping agents is currently in progress.

### Acknowledgements

We are thankful to the Volkswagen Foundation for financial support of our research.

### References

1. (a) Lee, J. G.; Park, J. Y.; Oh, Y. J.; Kim, C. S. *J. Appl. Phys.* **1998**, *84*, 2801. (b) Kodama, T.; Kitayama, Y.; Tsuji, M.; Tamaura, Y. *J. Magn. Soc. Jpn.* **1996**, *20*, 305. (c) Cornell, R. M. and Schwertmann, U. *The Iron Oxides*, VCH Publishers, Weinheim, 2nd ed., 2003.
2. (a) Tiefenauer, L. X.; Tschirky, A.; Kühne, G.; Andres, R. Y. *Magn. Res. Im.* **1996**, *14*, 391. (b) Gupta, A. K. and Gupta, M. *Biomater.* **2005**, *26*, 3995. (c) Mornet, S. and Vasseur, S. *J. Mater. Chem.* **2004**, *14*, 2161. (d) Duguet, E. and Vasseur, S. *Nanomedicine*, **2006**, *1*, 157.
3. Cabuil, V.; Neveu, S.; Rosenzweig, R. E. *J. Magn. Magn. Mater.* **1993**, *122*, 437.
4. (a) Sun, S. H. and Zeng, H. *J. Am. Chem. Soc.* **2002**, *124*, 8204. (b) Si, S. and Kotal, S. A. *Chem. Mater.* **2004**, *16*, 3489.
5. (a) Pedro, T. *J. Phys. D: Appl. Phys.* **2003**, *36*, 182. (b) Vayssieres, L.; Hagfeldt, A. and Lindquist, S. E. *Pure Appl. Chem.*, **2000**, *72*, 47.
6. (a) Willis, A. L.; Chen, Z. Y.; He, J.; Zhu, Y.; Turro, N. J. and O'Brien, S. *J. Nanomat.* **2007**, DOI: 10.1155/2007/14858. (b) Rockenberger, J.; Scher, E. C. and Alivisatos, A. P. *J. Am. Chem. Soc.* **1999**, *121*, 5608. (c) O'Brien, S.; Brus, L. and Murray, C. B. *J. Am. Chem. Soc.* **2001**, *123*, 12085.
7. (a) Klug, K. L.; Dravid, V. P.; Johnson, D. L. *J. Mater. Res.* **2003**, *18*, 988. (b) Sun, S. *J. Am. Chem. Soc.* **2003**, *126*, 273. (c) Yu, W. W.; Falkner, J. C.; Yavuz, C. T. and Colvin, V. L. *Chem. Commun.* **2004**, 2306.
8. Bronstein, L. M. and Huang, X. L. *Chem. Mater.* **2007**, *19*, 3624.
9. Yu, W. W. and Peng, X. *Angew. Chem.* **2002**, *41*, 2368.
10. Yin, M. and Chen, Z. Y. *J. Mater. Res.* **2007**, *22*, 1987.
11. Meyer, F.; Hempelmann, R.; Mathur, S. and Veith, M. *J. Mater. Chem.* **1999**, *9*, 1755.
12. Haas, M. and Mathur, S. unpublished work.
13. Park, J.; An, K.; Hwang, Y.; Park, J. G.; Noh, H. J.; Park, J. Y.; Hwang, J. H. and Hyeon, T. *Nature Mater.* **2004**, *3*, 891.

- 1  
2  
3  
4  
5  
6  
7  
8  
9  
10  
11  
12  
13  
14  
15  
16  
17  
18  
19  
20  
21  
22  
23  
24  
25  
26  
27  
28  
29  
30  
31  
32  
33  
34  
35  
36  
37  
38  
39  
40  
41  
42  
43  
44  
45  
46  
47  
48  
49  
50  
51  
52  
53  
54  
55  
56  
57  
58  
59  
60
14. Mathur, S. and Shen, H. "Inorganic Nanomaterials from Molecular Templates" in *Encyclopedia of Nanoscience and Nanotechnology*<sup>®</sup> Ed. by Nalwa, H. S. American Scientific Publisher, Vol. 4, p.131, 2004.

### Figure Captions

Figure 1. Processing diagram of  $\text{CoFe}_2\text{O}_4$  nanoparticles from single source precursor  $\text{CoFe}_2(\text{O}^t\text{Bu})_8$ .

Figure 2. (a) TEM and (b) HR-TEM images of cobalt ferrite nanoparticles by single source method.

Figure 3. Powder X-ray diffractogram of  $\text{CoFe}_2\text{O}_4$  nanoparticles obtained by thermal decomposition of  $\text{CoFe}_2(\text{O}^t\text{Bu})_8$ .

Figure 4. (a) TG curves showing the weight loss characteristic of several precursors upon thermal decomposition. (b) DSC curves for the comparison of single- and multi-source systems recorded with a heating rate of 10 K/minute under argon atmosphere.

Figure 5. TEM image of cobalt and iron oxide nanoparticles by multi-source method.

Figure 1

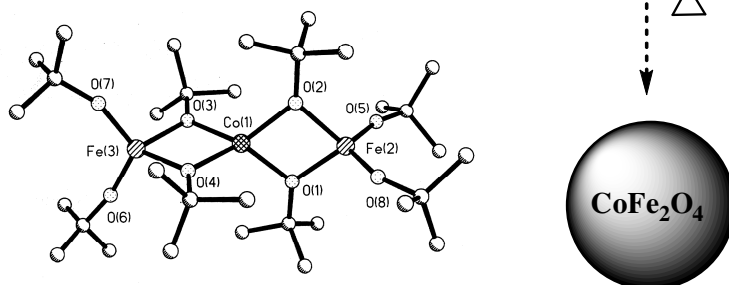


Figure 2a

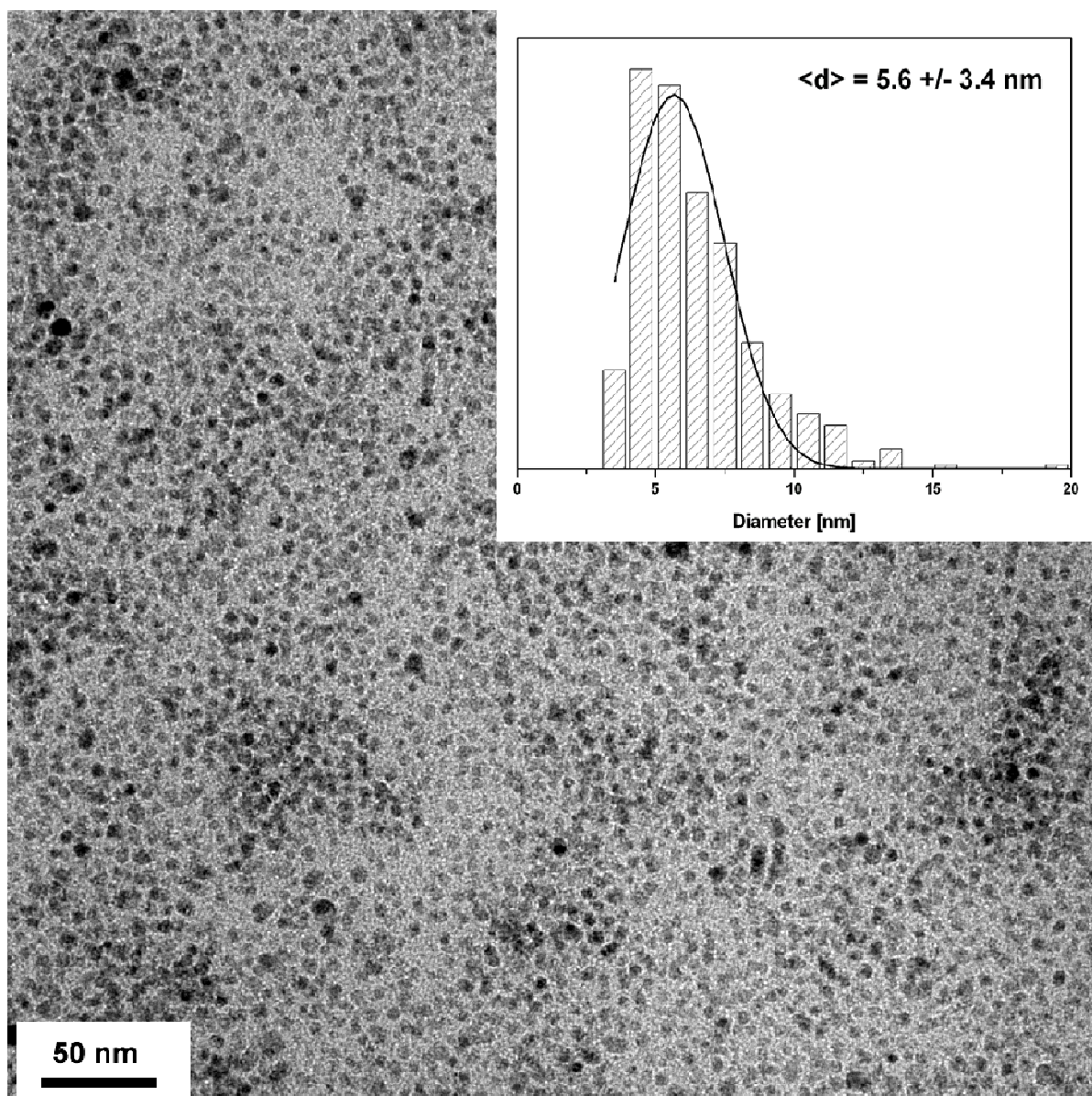


Figure 2b

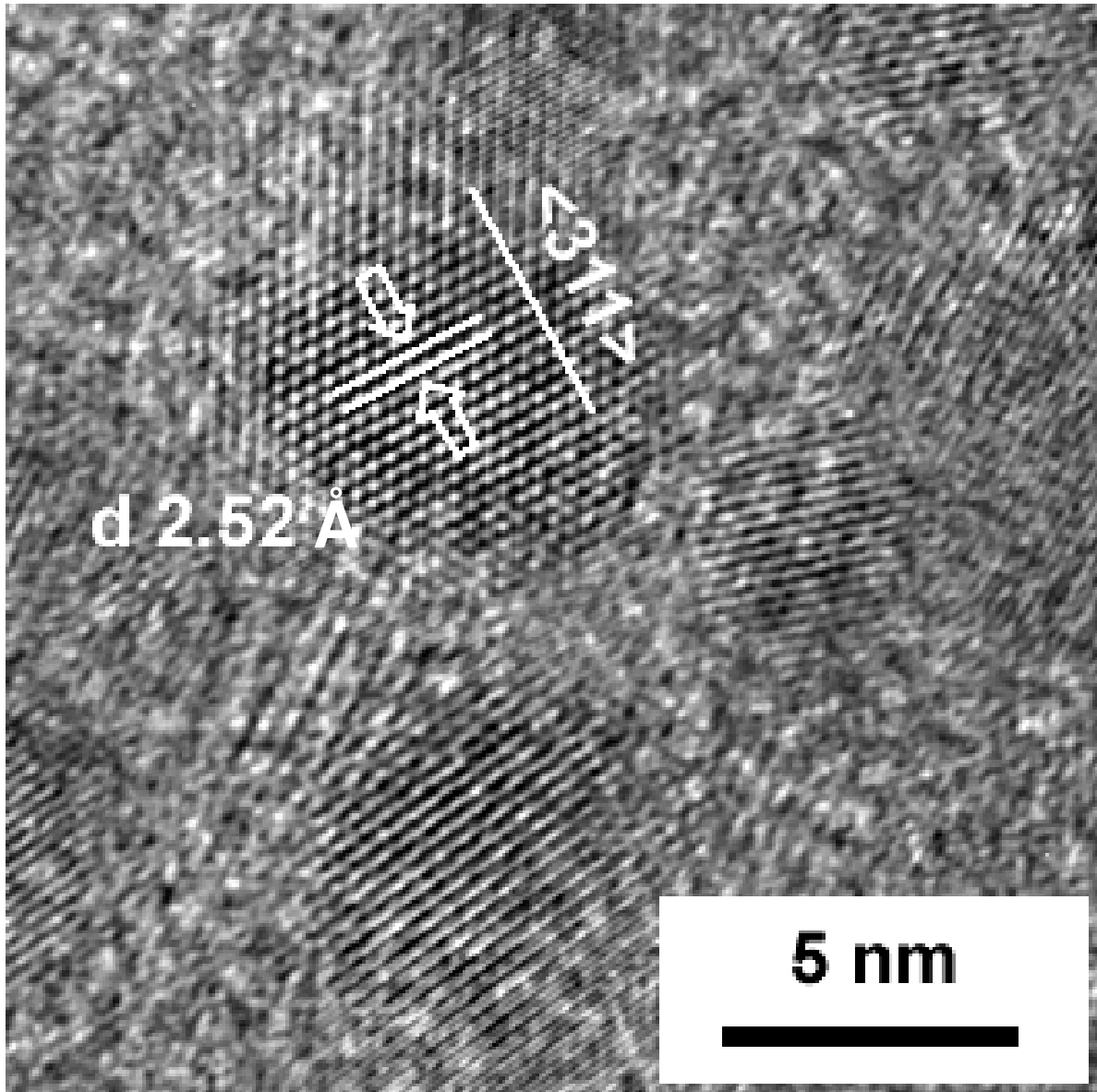


Figure 3

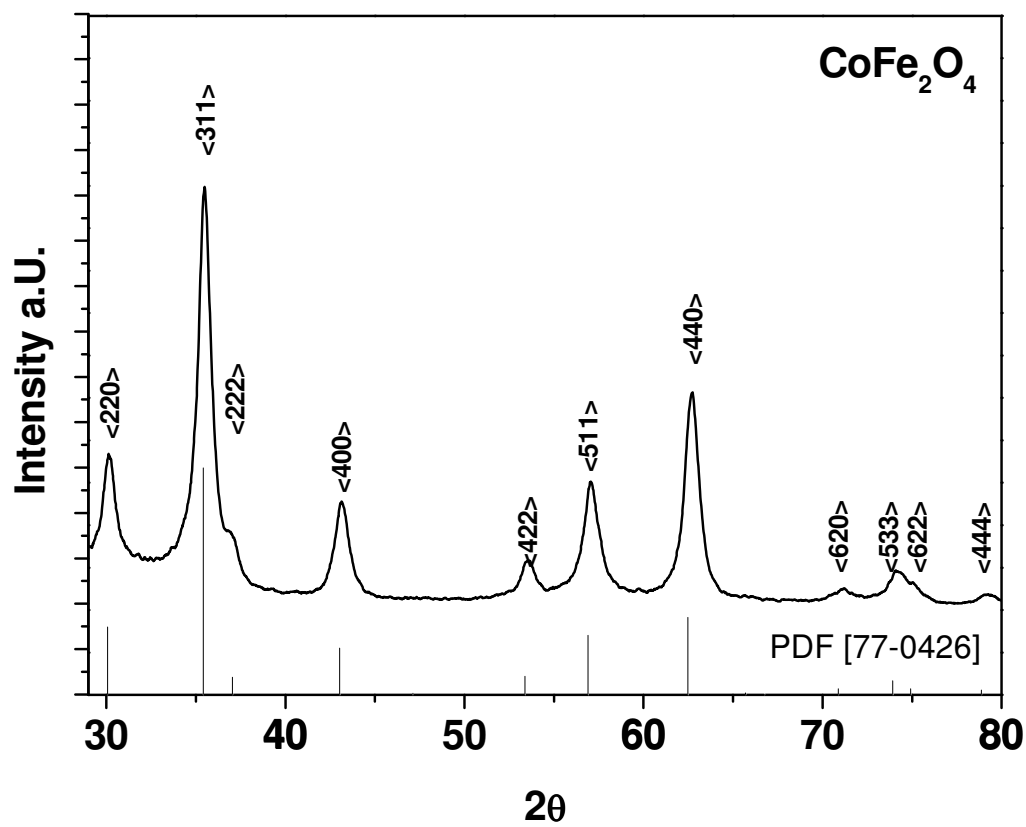


Figure 4a

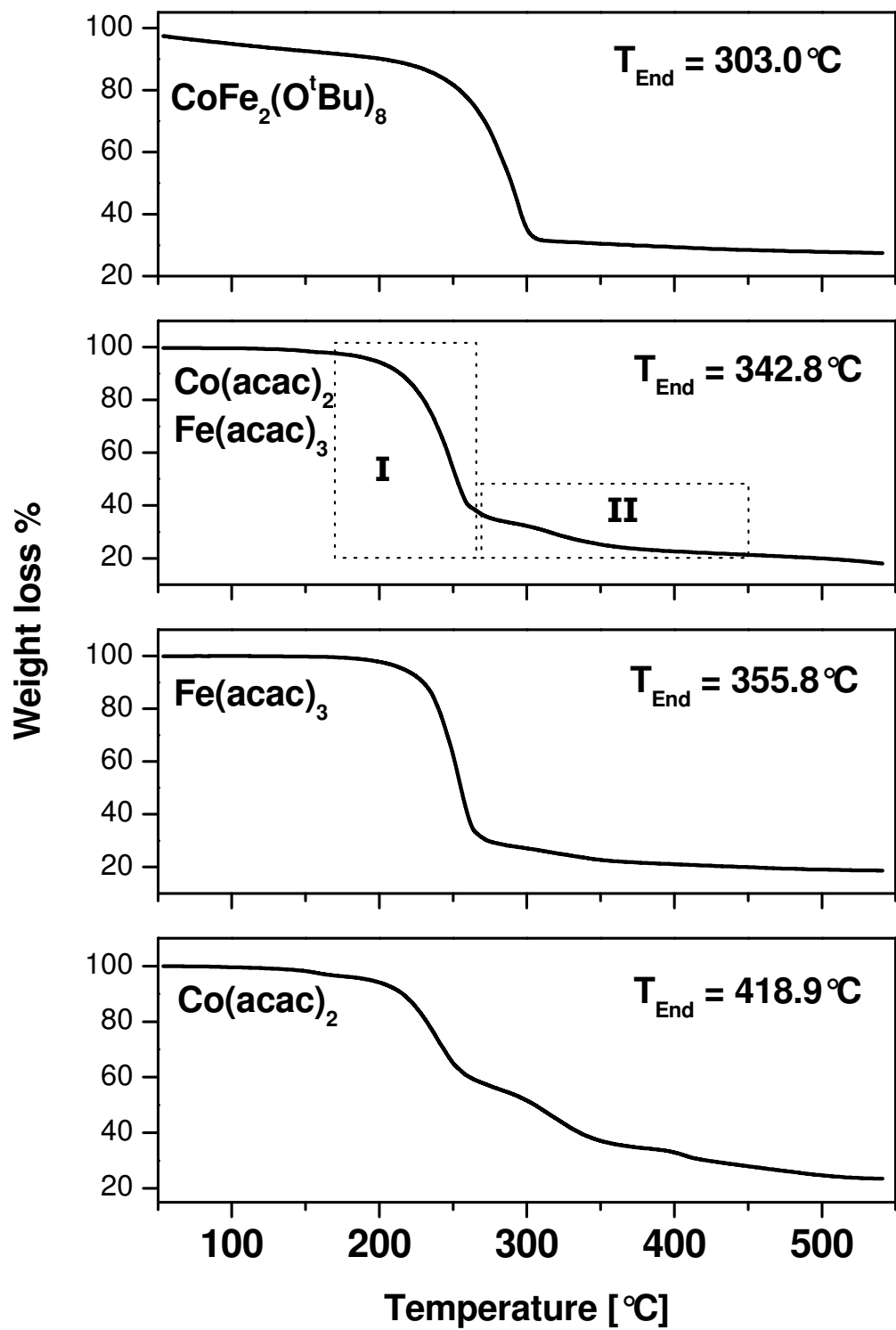


Figure 4b

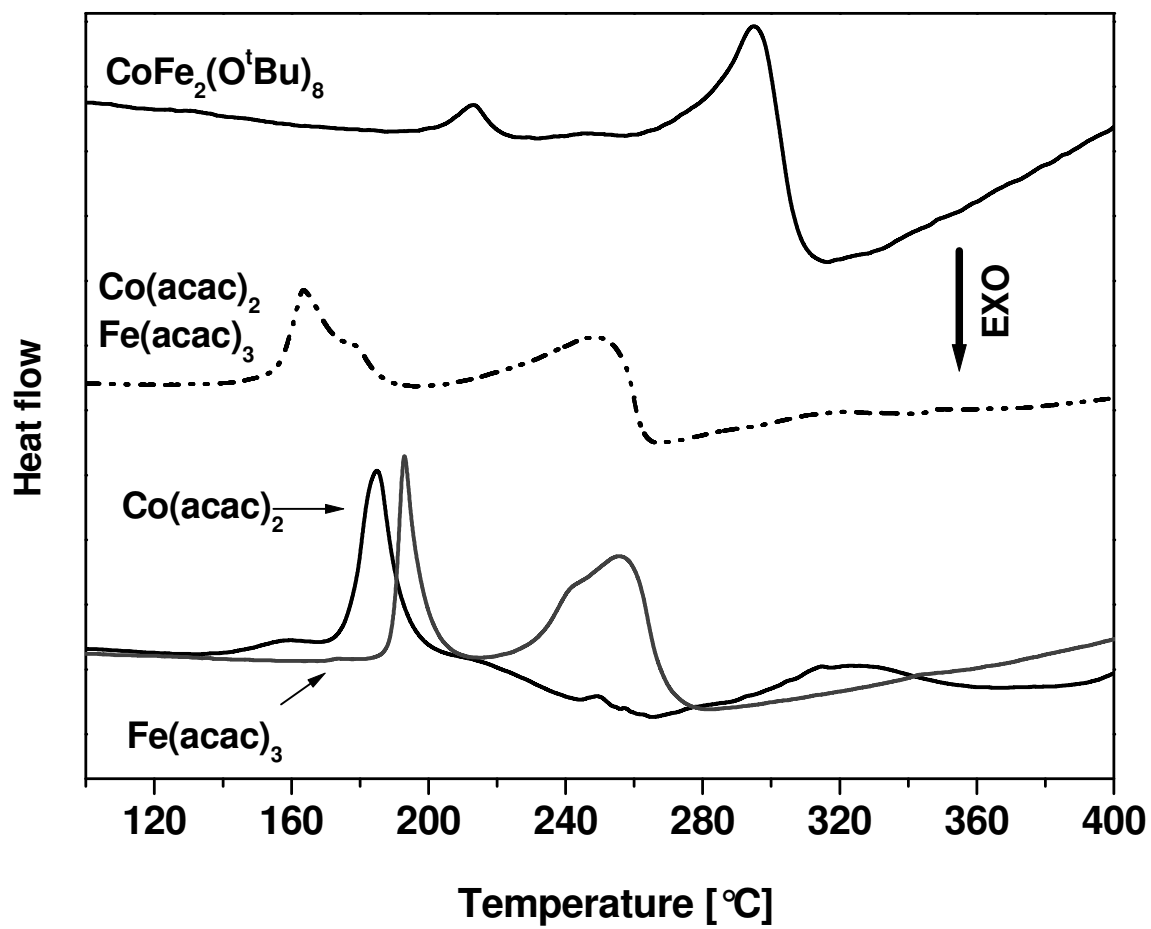


Figure 5

